Transport processes at fluidic interfaces
DFG SPP 1506

Analyse und Verständnis lokaler drei-dimensionaler Effekte bei der Taylor-Strömung in einem quadratischen Mini-Kanal

C. Falconi[1#], C. Lehrenfeld[2&], H. Marschall[3], C. Meyer[4], D. Bothe[3], A. Reusken[2], M. Schlüter[4], M. Wörner[1]

[1]Karlsruher Institut für Technologie, [2]RWTH Aachen, [3]TU Darmstadt, [4]TU Hamburg-Harburg
aktuelle Adressen: [#]Automotive Simulation Center, Stuttgart; [&]Technische Universität Wien

ProcessNet Fachausschusssitzung CFD und Mehrphasenströmungen
19.-20. März 2015, Lüneburg

Outline

- Introduction
- Experiment
- Numerical simulations
- Results
- Discussion
- Conclusions

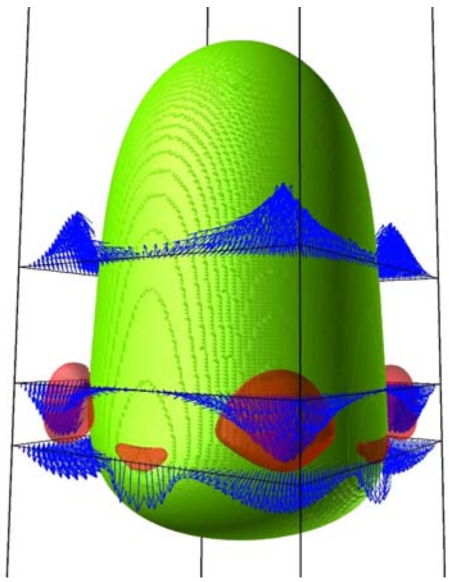

Guiding measure Taylor flow

- Taylor flow in millimeter size channels is of practical technical relevance and of fundamental physical interest
- Goal: Provide detailed experimental data under well controlled conditions which allow for a **quantitative validation** of numerical methods and computer codes
- Three cases from two experimental groups
  - **TBCC** = **T**aylor **B**ubble **C**ircular **C**hannel
    Boden et al. Exp Fluids 55 (2014) 1
    Aland et al. Int J Num Meth Fluids 73 (2013) 344
  - **TBSC** = **T**aylor **B**ubble **S**quare **C**hannel
    Boden et al. Exp Fluids 55 (2014) 1
    Marschall et al. Comp Fluids 102 (2014) 336
  - **TFSC** = **T**aylor **F**low **S**quare **C**hannel
    Meyer et al. Int J Multiph Flow 67 (2014) 140
    Falconi et al. Phys Fluids submitted

Taylor bubble

HZDR
(group Hampel)

Taylor flow

TUHH
(group Schlüter)

Taylor flow experiment

Geometry	Square vertical mini-channel (2.1 mm side length)	
Flow direction	Co-current upward	
Gas phase	Air	
Liquid phase	Water/glycerol mixture	
Gas volume fraction	0.37±0.02	
Bubble length	3.26±0.18 mm	
Liquid slug length	1.33±0.09 mm	
Unit cell length	4.59±0.27 mm	
Bubble velocity	135.9±1.9 mm/s	
Capillary number	0.1	$Ca = U_B \mu_L / \sigma$
Reynolds number	7.0	$Re = \rho_L D_h U_B / \mu_L$
Measurements	Velocity field in liquid slug and liquid film (µPIV) Estimation of bubble shape from µPIV observations	

This very regular Taylor flow is realized by a special injection valve combined with a compensation pipe for eliminating pressure fluctuations

Meyer, Hoffmann, Schlüter, Int J Multiph Flow 67 (2014) 140–148

Experiment

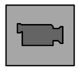

- Refractive index matching

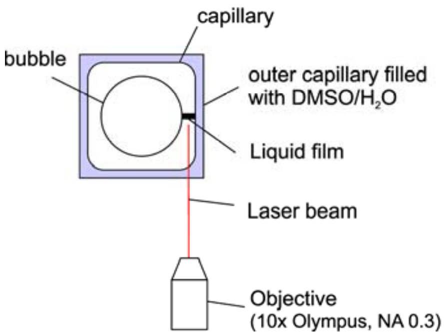

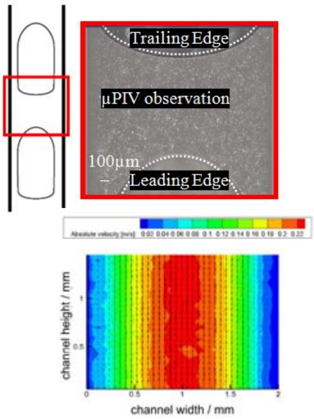

Meyer, Hoffmann, Schlüter, Int J Multiph Flow 67 (2014) 140–148

Equations and computer codes

- Single-field formulation for two immiscible Newtonian fluids with constant density, viscosity and surface tension (sharp interface limit)

$$\nabla \cdot \mathbf{u} = 0, \quad \partial_t(\rho \mathbf{u}) + \nabla \cdot (\rho \mathbf{u}\mathbf{u}) = -\nabla p + \nabla \cdot \eta \left(\nabla \mathbf{u} + (\nabla \mathbf{u})^{\mathrm{T}} \right) + \rho \mathbf{g} + \underbrace{\sigma \kappa \mathbf{n}_\Sigma \delta_\Sigma}_{=\mathbf{f}_\Sigma}$$

- Three academic in-house codes for 3D interface capturing
  - FS3D (ITLR Stuttgart, TU Darmstadt)
    - Volume-of-Fluid method (PLIC geometrical reconstruction, split advection)
    - Finite volume discretization on fixed staggered Cartesian grid
    - Advanced surface tension force model (balanced CSF)
  - TURBIT-VOF (KIT)
    - Similar to FS3D but un-split advection and less advanced surface tension model
  - DROPS (RWTH Aachen)
    - Level-set method with reinitialization
    - Finite element method with adaptive multilevel mesh hierarchy
    - Laplace Beltrami technique for surface tension, discontinuous pressure field

Marschall et al. Computers & Fluids 102 (2014) 336–352

Computational set-up

- From experiment
  - Side length D_h = 2.076 mm
  - Unit cell length L_{UC}= 4.59 mm
  - Gas volume fraction ε = 0.375
- Target value for simulations
  - Experimental bubble velocity
  - Simulations are transient but only quasi-steady results are analyzed here

Physical properties	Liquid	Gas
Density [kg/m^3]	1197.2	1.3
Viscosity [kg/ms]	0.0481	2×10^{-5}
Surface tension [N/m]	0.0624	

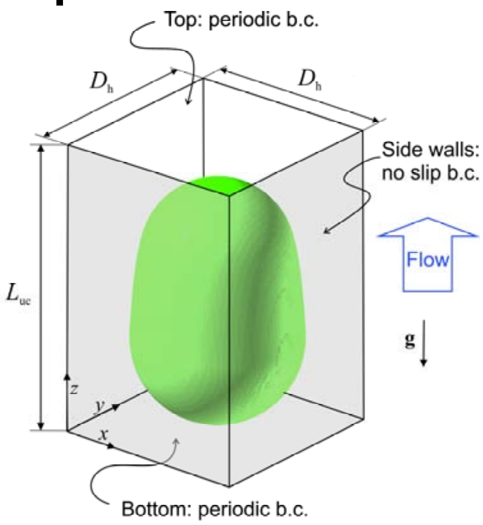

Grid and integral simulation results

	FS3D	TUV	DROPS	Dev$_C$ [%]	Exp.	Dev$_E$ [%]
Domain	V_{UC} / 4	V_{UC}	V_{UC} / 8			
Grid* (for V_{UC})	64×64×128	100×100×220	64×64×128			
U_B [mm/s]	135.9	135.9	135.0	**0.4**	135.9±1.9	**0.2**
L_B [mm]	3.355	3.328	3.329	**0.5**	3.26±0.18	**2.4**
L_S [mm]	1.235	1.262	1.261	**1.4**	1.33±0.09	**5.8**
$\Delta p/L_{UC}$ [Pa]	117.8	119.2	121.2	**1.5**		
J [mm^3/s]	377.2	391.6	382.6	**2.0**		

J = total superficial velocity (volumetric flow rate of the two-phase flow)

*Grid resolution corresponds to about 3 mesh cells per lateral film width (smallest length scale of the flow)

$$\mathrm{Dev}_C = \frac{\mathrm{Max}_{i=1-3}\left|CFD_i - CFD_{\mathrm{mean}}\right|}{CFD_{\mathrm{mean}}}, \quad \mathrm{Dev}_E = \frac{\left|Exp - CFD_{\mathrm{mean}}\right|}{Exp}$$

Bubble shape

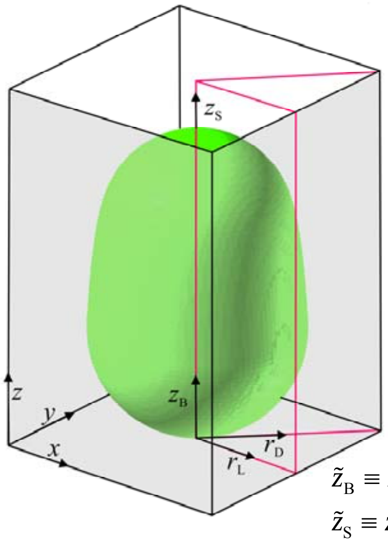

$\tilde{z}_B \equiv z_B / L_B$

$\tilde{z}_S \equiv z_S / L_S$

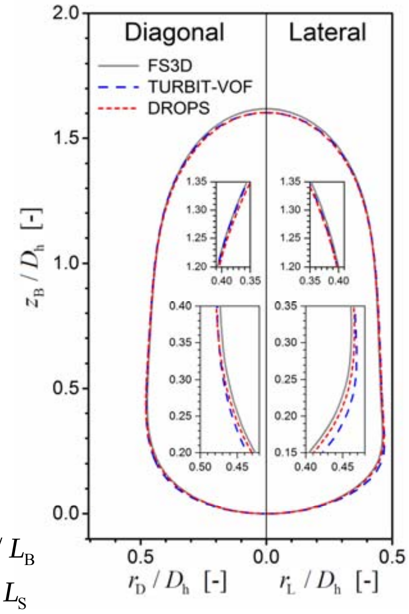

Quantitative comparison of bubble shape

	Cut	z_B/L_B [-]	FS3D	TUV	DROPS	Dev_C [%]	Exp.	Dev_E [%]
Bubble radius [μm]	L	0.25	952	961	960	0.6	946±8	1.2
		0.5	918	925	922	0.4	940±8	2.0
		0.75	824	825	824	0.1	847±8	2.7
	D	0.25	983	991	993	0.6		
		0.5	949	953	954	0.3		
		0.75	839	845	839	0.5		
Film thickness [μm]	L	0.25	86	77	78	7.1	92±8	12.7
		0.5	120	113	116	3.2	98±8	18.7
		0.75	214	213	214	0.3	191±9	11.9
	D	0.25	485	477	475	1.3		
		0.5	519	515	514	0.6		
		0.75	629	623	629	0.6		
Extreme value	L	z_B/L_B	0.198	0.173	0.194	1.5		
		$R_{B,max-L}$	959	973	967	0.8		
		$\delta_{F,min-L}$	79	65	71	10.3		
	D	z_B/L_B	0.273	0.270	0.275	0.3		
		$R_{B,max-D}$	985	991	994	0.5		
		$\delta_{F,min-D}$	483	477	474	1.1		

Velocity profiles in liquid slug

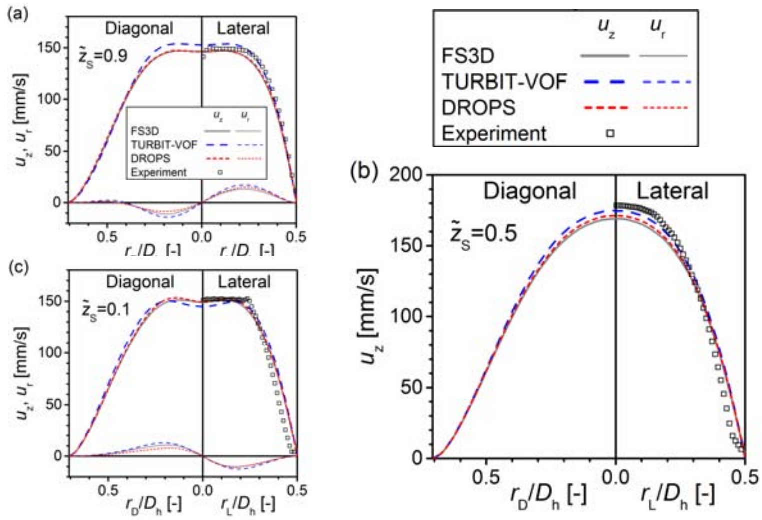

Velocity profiles in bubble and film

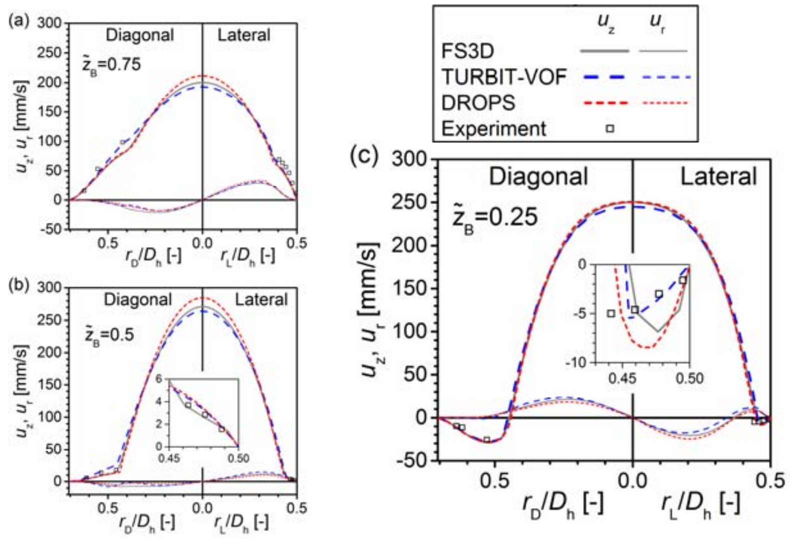

Quantitative comparison of velocity profiles

- Centerline axial velocity

	z_S/L_S [-]	FS3D	TUV	DROPS	Dev_C [%]	Exp.	Dev_E [%]
Liquid slug [mm/s]	0.9	146.4	152.7	146.1	**2.9**	141.3	**5.0**
	0.5	169.0	174.8	171.2	**1.8**	178.3	**3.7**
	0.1	148.9	144.9	149.0	**1.8**	151.2	**2.4**
	z_B/L_B [-]						
Bubble [mm/s]	0.75	199.0	192.8	211.46	**5.2**		
	0.5	270.9	264.0	284.7	**4.2**		
	0.25	250.6	245.0	250.6	**1.5**		

Flow field (Results of FS3D)

- Streamlines (moving ref. frame)
  - Gas phase
    - One main vortex
    - Two counter-rotating vortices at bubble nose and rear
    - Positions of center of main vortex is different in lateral and diagonal cut → flow in bubble is three-dimensional
  - Liquid phase
    - Region with circulation flow (channel center) and bypass flow (near wall) are separated by the dividing streamline
- Vertical velocity u_z (fixed frame)
  - Regions with negative velocity in rear part of the liquid film → local backflow

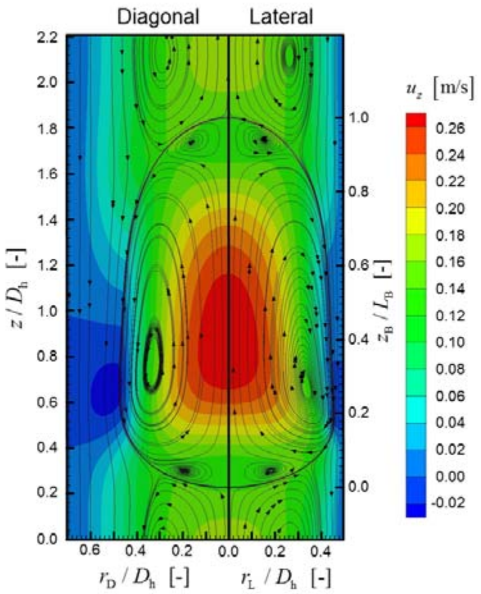

Local backflow in liquid film

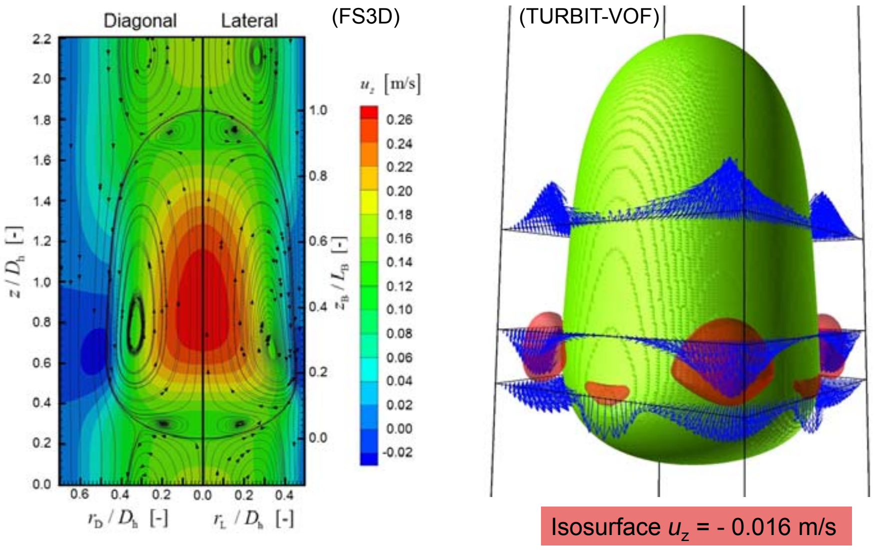

Local backflow in co-current flow

- Local backflow results in a temporal inversion of the wall shear stress at a fixed position during passage of a Taylor bubble
  - Important for various applications with Taylor flow
    - Heat and mass transfer
    - Cleaning of membranes for ultrafiltration
    - Synthesis of nanoparticles
    - Biological and medical applications with living cells
- Literature status
  - The phenomenon of possible shear stress reversal is known for some time
  - Local backflow in co-current Taylor flow has not been measured before
  - It has been found in computations for circular tubes
    S.P. Quan, Co-current flow effects on a rising Taylor bubble, IJMF 37 (2011) 888
- Questions related to present results for square channel
  - Why differ axial locations with backflow in lateral film and corner region?
  - Can we give criteria when this newly discovered phenomenon occurs?

Sufficient condition for backflow

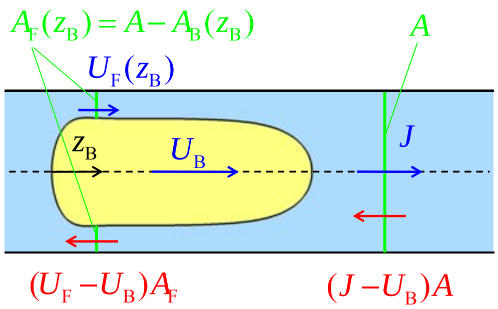

J = total superficial velocity of the Taylor flow
U_F = mean axial velocity in liquid film at position z_B

- Liquid mass balance in moving frame of reference yields

$$\dot{V}_{L,mfr} = (J - U_B)A = \left[U_F(z_B) - U_B\right]A_F(z_B)$$

Sufficient condition for backflow

- From liquid mass balance it follows

$$\frac{U_F(z_B)}{J} = \frac{1 - \frac{U_B}{J}\frac{A_B(z_B)}{A}}{1 - \frac{A_B(z_B)}{A}} \quad \Rightarrow \text{ backflow occurs where } \quad \frac{U_B}{J}\frac{A_B(z_B)}{A} > 1$$

- For an axisymmetric bubble it is

$$U_F(z_B) = \frac{J - U_B \frac{\pi}{4}\frac{D_B^2(z_B)}{D_h}}{1 - \frac{\pi}{4}\frac{D_B^2(z_B)}{D_h^2}}$$

- This relation can be used to compute the mean velocity in the liquid film, U_F, from the axial profile of the bubble diameter

Evaluation from L/D bubble profiles

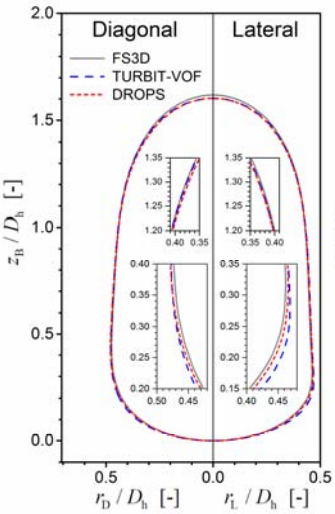

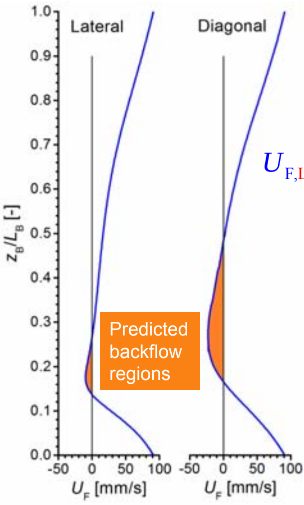

$$U_{F,L/D} = \frac{J - U_B \frac{\pi}{4} \frac{D_{B,L/D}^2}{D_h}}{1 - \frac{\pi}{4} \frac{D_{B,L/D}^2}{D_h^2}}$$

- Predicted regions with backflow differ as observed
- L/D profiles differ → bubble is not axisymmetric. Why?

Bubble aspect ratio

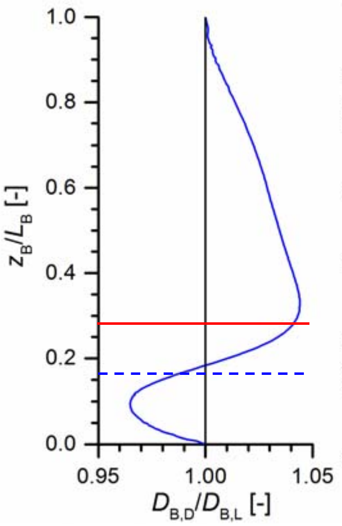

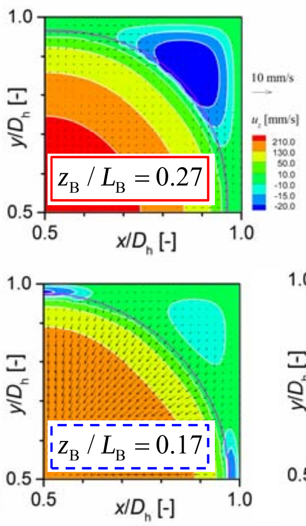

Minimum diagonal film thickness

Minimum lateral film thickness

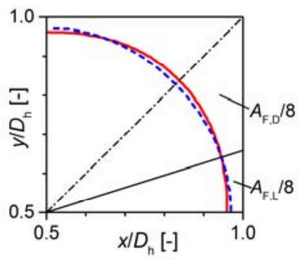

Pressure field (Results of TURBIT-VOF)

- Non-dimensional (periodic) pressure field in two horizontal cross-sections
- In front part of the bubble the pressure is higher in the lateral film than in the corner film
- In the rear part of the film it is opposite

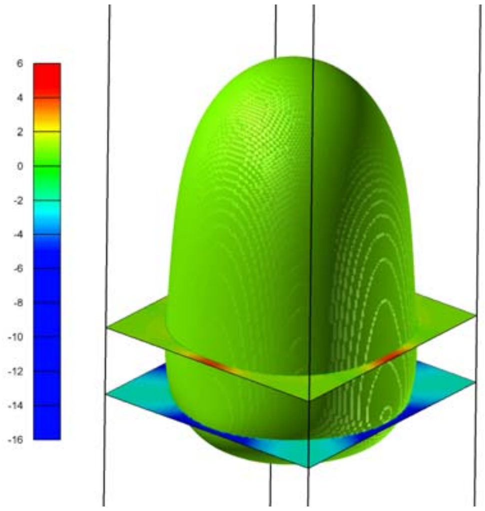

Force balance normal to the interface

- Local force balance normal to the interface in a horizontal cross-section

$$-(p_L - p_G) + \left[\mu_L\left(\nabla \mathbf{v}_L + \nabla \mathbf{v}_L^{\mathrm{T}}\right) - \mu_G\left(\nabla \mathbf{v}_G + \nabla \mathbf{v}_G^{\mathrm{T}}\right)\right] : \hat{\mathbf{n}}_L \hat{\mathbf{n}}_L = 2H\sigma$$

- Neglecting normal viscous stresses
  $\Rightarrow$ the pressure jump is locally balanced by capillary forces

$$p_G - p_L \approx 2H\sigma \qquad \sigma = const. \qquad p_G = p_{\mathrm{B}} \approx const.$$

- For the given azimuthal variation of p_{L} this can only be achieved by a change of the local interface curvature

$$H = \frac{1}{2}\left(\frac{1}{R_{\min}} + \frac{1}{R_{\max}}\right) \approx \frac{p_B - p_L}{2\sigma}$$

- This causes the deviation of the bubble shape from rotational symmetry

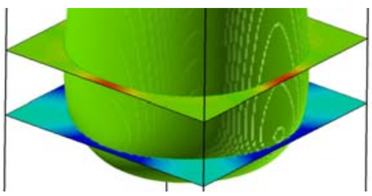

Refined liquid mass balance analysis

- Splitting the liquid flux into two parts through lateral and diagonal film

$$(J - U_B)A = \left[U_{F,L}(z_B) - U_B\right] A_{F,L}(z_B) + \left[U_{F,D}(z_B) - U_B\right] A_{F,D}(z_B)$$

- We are interest in the position where the axial velocity in L/D film is minimal → derivative with respect to z_B gives

$$A_{F,L}\frac{\partial U_{F,L}}{\partial z_B} + A_{F,D}\frac{\partial U_{F,D}}{\partial z_B} = \underbrace{\left[U_B - U_{F,D}(z_B)\right]}_{\approx U_B}\frac{\partial A_{F,D}}{\partial z_B} + \underbrace{\left[U_B - U_{F,L}(z_B)\right]}_{\approx U_B}\frac{\partial A_{F,L}}{\partial z_B}$$

$$A_{F,D}\frac{\partial U_{F,D}}{\partial z_B} \approx U_B\frac{\partial A_F}{\partial z_B} - A_{F,L}\frac{\partial U_{F,L}}{\partial z_B}$$

$$A_F = A_{F,L} + A_{F,D}$$

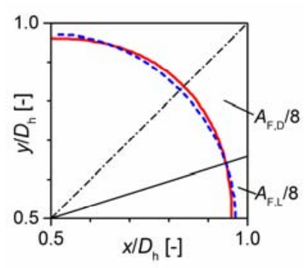

Refined liquid mass balance analysis

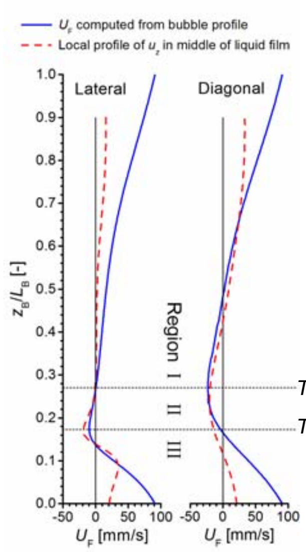

Thinnest diagonal film

Thinnest lateral film

$$\underbrace{A_{F,D}}_{>0}\frac{\partial U_{F,D}}{\partial z_B} \approx \underbrace{U_B}_{>0}\frac{\partial A_F}{\partial z_B} - \underbrace{A_{F,L}}_{>0}\frac{\partial U_{F,L}}{\partial z_B}$$

	$\frac{\partial A_F}{\partial z_B}$	$\frac{\partial U_{F,L}}{\partial z_B}$	$\frac{\partial U_{F,D}}{\partial z_B}$
Region I	>0	>0	>0
Region II	>0 =0 <0	>0 >0 >0	? <0 <0
Region III	<0	<0	<0

cf. local profiles of u_z

- In the lower part of region II the derivatives have opposite signs so that the position of velocity minimum in the L and D film differ

Approximate criteria for backflow

- Backflow occurs for

$$\underbrace{\frac{U_B}{J}}_{>1}\underbrace{\frac{A_B}{A}}_{<1} > 1$$

Both ratios depend on the capillary number

$$Ca \uparrow \quad \frac{U_B}{J} \uparrow \quad \frac{A_B}{A} \downarrow$$

- Circular channels
  - Correlation of Liu et al. (2005) or Abiev (2013) for U_B/J
  - Correlation of Aussilious & Quere (2000) for $\delta_F \rightarrow A_B/A$
- Square channels
  - Correlation of Liu et al. (2005) for U_B/J
  - Correlation of Kreutzer et al. (2005) for D_B, $D_L \rightarrow A_B/A$
  - If the Taylor bubble is not axisymmetric then the local backflows in the lateral and diagonal film occur in different axial regions
  - Transition occurs at $Ca \approx 0.04 - 0.1$ (for larger values bubble is axisymm.)

Conclusions and outlook

- Quantification of relative deviations between codes
  - Bubble diameter 0.6% ✓
  - Minimum liquid film thickness 10% (model for surface tension force ×)
  - Centerline velocity liquid slug 3% (✓)
  - Centerline velocity within bubble 5% ×
- Analysis of local backflow in rear part of the liquid film
  - Temporal reversal of wall shear stress during passage of a Taylor bubble
  - Location of backflow region in lateral and diagonal film (square channel)
    - For non-axisymmetric bubbles, the local backflow occurs at different axial positions in the lateral and corner film
    - Reason: a cross-over of the diagonal/lateral bubble aspect ratio
    - Variation of bubble aspect ratio has strong implications on local flow in rear film
  - Approximate criteria when phenomena may occur in practice
- Outlook
  - Influence of *Ca* and *Re* on size of backflow region
  - Trapezoidal and triangular channels

We gratefully acknowledge the funding by the DFG

Thank you for your attention!